sustainability

MDPI

Article

Utilizing the Harvesting of Rainwater to Provide Safe Road Transportation Efficiency and Increase Water Resources in the Context of Climatic Change

Mohamed Elsayed Gabr [1,*], Amira Mahmoud El Shorbagy [1,2,*] and Hamdy Badee Faheem [3]

[1] Civil Engineering Department, Higher Institute for Engineering and Technology, Ministry of Higher Education, New Damietta 12588, Egypt
[2] Civil Engineering Department, Faculty of Engineering, Minia University, Minia 61519, Egypt
[3] Highway and Traffic Engineering, Civil Engineering Department, Faculty of Engineering, Minia University, Minia 61519, Egypt
[*] Correspondence: mohamed.gabr@ndeti.edu.eg (M.E.G.); mamera715@gmail.com (A.M.E.S.)

Abstract: This research investigates the effect of heavy rain on highway traffic volume and average speed, and proposes a recharging well harvesting system as an alternative freshwater source in the context of climate change. The Cairo Autostorad highway was taken as a case study. The highway climate data were collected, and traffic was measured using Metrocount equipment during the period from 2008 to 2020. The results show that the studied road is about 12 km long, and about 40 water ponds exist along the route. Each pond has an estimated water volume of 300 m^3, and a 30 cm recharging well, with a maximum recharging capacity of 25 m^3/h with satisfactory performance, is recommended to be constructed for rainwater harvesting. The recharging wells will clear the ponding volume within 2.5 to 3.5 h after the rainfall has stopped. The design incorporates a 1.2 safety factor against blockage inside the well. In addition, a model was established between the average rainfall depth and the average measured highway speed for the period (2008–2020) during rainy months, indicating an exponential function with a determination factor R^2 = 0.7076. The present rainfall (2020) and the representative concentration path (RCP) for 4.5 and 8.5 emissions scenarios were used to simulate the rainfall for future years: the 2040s, 2060s, 2080s, and 2100s. The results show that in the winter season for the current scenario (2020), the average rainfall depth was 45 mm, and the highway speed was 78 km/h. For the RCP 4.5 emission scenarios for the 2040s, 2060s, 2080s, and 2100s, the rainfall depths were 67.8, 126.4, 131.2, and 143.9 mm, and the corresponding reductions in the highway speeds were 23, 34, 35.3, and 36.9%, respectively, compared to the baseline scenario (2020). On the other hand, the RCP 8.5 emission scenarios show a reduction in the highway speed of 23, 34.5, 36.9, and 36.9% for the years 2040, 2060, 2080, and 2100, respectively, due to rainfall depths of 68.7, 128.4, 143.9, and 143.9 mm, respectively. This study helps policymakers to make wise decisions regarding sustainable water resource management and highway traffic problems related to rainwater depths in the context of climate change.

Keywords: climate change; rainwater harvesting; highway traffic; recharging well; highway speed

check for updates

Citation: Gabr, M.E.; El Shorbagy, A.M.; Faheem, H.B. Utilizing the Harvesting of Rainwater to Provide Safe Road Transportation Efficiency and Increase Water Resources in the Context of Climatic Change. *Sustainability* **2022**, *14*, 9656. https://doi.org/10.3390/su14159656

Academic Editors: Elżbieta Macioszek, Margarida Coelho, Anna Granà and Raffaele Mauro

Received: 11 July 2022
Accepted: 3 August 2022
Published: 5 August 2022

1. Introduction

Climate change is expected to influence urban living conditions and challenge the ability of cities to adapt and mitigate climate change [1]. The lifelines of socioeconomic and sustainable development in metropolitan areas are water and roads. Road transportation is a necessary component part of a nation because it is utilized to support social and economic activity more than any other mode of transportation; infrastructure is sometimes referred to as its socio-economic lifeline [2]. A road transportation system is made up of facilities and activity zones. When the sky is covered in smoke, dust, rain, snow, or fog, driving becomes more difficult [3]. Due to the varied driving styles of drivers in diverse weather circumstances, weather conditions have had a considerable influence on the functioning of the road network since the middle of the 20th century [4]. The coupled Model Intercomparison Project (CMIP) is used by the World climate Research Program (WCRP), the working group responsible for modeling the Intergovernmental Panel on climate change (IPCC) [5]. These intercomparisons look at a large number of models from a variety of modeling centers throughout the world, examining a wide range of model behaviors and evaluating each model's strengths and flaws through controlled tests. These tests aid in the detection of faults that are exclusive to a single model or that may necessitate a broad theoretical modification. In experiments, "near-term" trends over a 10- to 30-year time frame and "long-term" patterns over a 100-year time horizon are examined [6]. The IPCC's most recent report employed an ensemble of fifty-five distinct climate models from the fifth phase of the CMIP, or CMIP5. A significant advancement in the prediction methodology used by the CMIP5 project is the categorization of future scenarios in terms of radiative forcings [7,8]. This idea, known as representative concentration pathways (RCP), defines four estimated greenhouse gas emission scenarios based on the social and political factors of implementing mitigation methods. The most optimistic criterion, RCP 2.6, assumes that annual global greenhouse gas (GHG) emissions will peak between 2010 and 2020, after which they will begin to decline. RCP 4.5 predicts a peak in emissions around 2040, followed by a decline. The RCP 8.5 results from insufficient efforts to cut emissions and is an example of how warming cannot be stopped by the year 2100. At the International Institute for Applied Systems Analysis (IIASA), Austria, the MESSAGE modeling team and the IIASA Integrated Assessment Framework produced the RCP 8.5 [9]. The RCP 8.5 represents scenarios that result in high greenhouse gas concentration levels and is defined by increasing greenhouse gas emissions over time. The RCP 4.5 and 8.5 emissions pathways are described in Table 1. The two scenarios have the radiative forcing topping at 4.5 and 8.5 Wm^{-2} by 2100, respectively.

Table 1. The representative concentration pathways description.

Name	CO_2 Equivalent (ppm)	Temperature Anomaly (°C)	Radiative Forcing	Pathway
RCP 4.5	650	2.4	4.5 Wm^{-2} post 2100	Stabilization without overshoot
RCP 8.5	1370	4.9	8.5 Wm^{-2} in 2100	Rising

Egypt's main source of water is the Nile River [10]. Therefore, any alterations in its flow are extremely crucial. The Nile River loses a considerable amount of water due to evaporation during its 3000 km length through arid northern Sudan and Egypt [11]. As a result, fluctuations in temperature and precipitation have a significant impact on the water supply. Mostafa et al. [12] determined in their analysis that due to the impact of climate change on water demand and withdrawals, groundwater supplies in Egypt's Nile valley and delta may be diminished. Changes in precipitation and runoff, as well as changes in use and withdrawal, have led to a reduction in surface and groundwater supplies in many places. Climate change, water, and agriculture may have a substantial interaction. Climate change might have a wide range of effects on water resources. Changes in precipitation amount and patterns are among these dimensions [12]. Extreme weather occurrences, such as floods and droughts, may also have an impact on water resources. Droughts and drier soils are likely in West Africa and the Amazon between the months of June and August, and in the Asian monsoon region during the months of December through February. These changes could have a significant impact on agricultural production and food security around the world [13]. In old cities, the quantities of rainfall will flow into the sewerage networks that are designed to drain only limited amounts of rainfall. In extreme rain events, the sewerage networks may be flooded, which may lead to ecological and economic hazards. Rainwater must be completely separated from the sewage networks because the influx of rainwater causes a burden on the sewage treatment plants, as well as a large loss of electrical energy during treatment, in addition to causing road traffic problems. Some coastal cities in Egypt have witnessed many cases of drowning, and every year, the rains always constitute a burden on the sewage stations. Rainwater harvesting (RH) is the collection, storage, distribution, and use of rainwater for a range of purposes, including drinking and domestic uses, irrigation, industry, and livestock grazing, as well as for reducing the load on sewage treatment plants [14–16]. RH in urban environments can be performed by using rainwater sewer networks to collect the rainwater from large surfaces and rooftops and store it in under- or aboveground tanks [17,18]. The construction cost of these tanks is extremely high, and the tanks require a significant amount of space and a complicated pumping system. Without RH, several negative consequences can occur, such as (i) decreased road efficiency and reliability [19], (ii) various pollutants (sediments, toxic chemicals, debris, nutrients, and litter) may be moved to nearby residential areas [20], (iii) anthropogenic pollutants, heavy metals, bird droppings, and animal waste can be transferred from roads and roofs into downstream water [21,22], and (iii) flows of stormwater runoff over urban impervious surfaces can cause flooding, traffic problems, and heavy casualties [23]. Accordingly, the life of urban dwellers, the aquatic environment, and hydrology can all be impacted [24]. In Egypt, however, there has been little research on rainwater harvesting in the coastal regions and the rain-related road conditions and driving behavior during severe weather. Despite the lack of studies on traffic flow characteristics and performance analyses in Egypt, the majority of traffic management strategies, traffic control techniques, and traffic designs for severe weather are developed and modified based solely on personal experience. This method is inefficient, since it requires a traffic operator to alter settings manually in the field, which has a significant impact on the traffic system's dependability and efficiency. Floods are one of the most hazardous natural catastrophes, since they may devastate any mode of transportation. Different flood effects on traffic flow characteristics may be noticed when floodwater blocks a portion of a route network, such as communication interruptions, traffic congestion, increased traffic volume, lowered speeds, and increased travel time [25]. Figure 1 shows the effect of rainfall on the road, and as a result, every effect on the route network can be viewed as a possible threat to the various characteristics of traffic flow. As a result, a solution to the problem of flooding must be devised by establishing an information system (IS) capable of visualizing the interaction between flood dimensions and route networks. Accordingly, it may be possible to comprehend the flood impact on an object, because flooding impact can be defined as the probability of contact between flood dimensions and real-world objects [26]. Furthermore, the system should be able to identify, classify, and evaluate the various levels of flood impact on the route network, as well as show them in both two and three dimensions [27]. This could allow for qualitative analysis and visualization of the physical impact of a flood on a route network. The system might be used to visualize the flood impact on traffic flow characteristics (traffic volume, journey time, speed) in both qualitative and quantitative ways because the flow of traffic (activities domain) is based on the availability of a route network. The information above could help to support decision-making processes aimed at reducing the impact of flooding on road transportation systems. As a result, the article details the creation of such a system as part of an advanced software life cycle [28]. The primary goal of this study is to assess the climatic changes in road traffic due to the excess rainfall and the harvesting of rainfall spatially in the coastal regions to solve traffic problems and increase freshwater resources in Egypt. To achieve the study objectives, (i) the previous work regarding the effect of climatic changes on road efficiency and rainfall intensity is reviewed, (ii) a case study for the Greater Cairo Metropolitan Area (GCMA), specifically the El Monib road intersection with the ring road, is analyzed, (iii) climate data for the current 2020 status and the RCP 4.5 and 8.5 emissions were collected for the 2040s, 2060s, 2080s, and 2100s, (iv) the Metrocount tool is used to measure the saturation flow rate, traffic volume, and road travel speed, (iv) data analyses and comparisons of road speed and volume under different weather conditions were carried out, (v) the identification of water pond was completed and sites maps were developed, and (vi) a method regarding rainwater harvesting is presented.

Figure 1. Some indicative photos of the road after a rainfall.

2. Materials and Methods

2.1. Study Area

More than one-fifth of Egypt's population lives in the Greater Cairo Metropolitan Area (GCMA), which is home to more than 28.7 million people. The GCMA contributes significantly to Egypt's economy in terms of GDP and employment. By 2027, the GCMA's population is anticipated to reach 40 million, indicating that the region will also become more economically significant. Traffic congestion is a big problem in the GCMA that has a severe impact on both the economy and the standard of living. Congestion consumes time that could be spent performing more beneficial activities, raises harmful emissions, decreases air quality, boosts corporate transportation costs, and deters businesses and industries from investing in the GCMA. The ring road in Cairo, which connects the city's heart to outlying areas, is an eight-lane free-for-all, with automobiles, buses, and heavy trucks flowing in and out at fast speeds. The data used in this study are obtained from the El Monib road to the intersection of the ring road with the Autostorad highway. This highway has 4 lanes, and its design speed is 90 km/h; the speed was observed using the Metrocount tube traffic flow collection system. The device can continuously observe traffic flow parameters, including flow, velocity, and density of the highway during the survey time period. Figure 2 illustrates the study area.

Figure 2. The study area.

2.2. Climate Change Models

Weather data regarding the road were collected from the Egyptian Meteorological Authority and www.tutiempo.net/clima RSMc-Cairo (http://web.civilaviation.gov.eg/companies/Meteorology) (assessed on 20 June 2022) for the period from 2008 to 2020. In addition, a number of climate models used are non-selective, i.e., we use as many models as are currently available to us, as listed in Table 2. We focus on RCP 4.5 and RCP 8.5, which are correspondingly medium-low and high radiative forcing scenarios. For the overconfidence of the lone model, multi-model joint projections are also created, as this comprises information from all contributing models. It is also supposed that multi-model ensembles are desirable to single models.

Table 2. The CMIP5 models used in this study.

Model	Model Institution	Resolution	Reference
CMCC-CMS	Centro Euro-Mediterraneo per I Cambiamenti Climatici, Italy	$1.9° \times 1.9°$	[29]
ACCESS1-0	Commonwealth Scientific and Industrial Research Organization/Bureau of Meteorology, Australia	$1.9° \times 1.3°$	[30]
CCSM4	National Center for Atmospheric Research	$0.9° \times 1.25°$	[31]
CNRM-CM5	Centre National de Recherches Meteorologiques	$1.4° \times 1.4°$	[32]
CSIRO-Mk3	Australian Commonwealth Scientific and Industrial Research Organization	$1.9° \times 1.9°$	[33]
CanESM2	Canadian Centre for Climate Modeling and Analysis	$2.8° \times 2.8°$	[34]
GFDL-CM3	Geophysical Fluid Dynamics Laboratory	$2.5° \times 2°$	[35]
HadGEM2-CC	Met Office Hadley Centre, UK	$1.9° \times 1.3°$	[36]
HadGEM2-ES	Met Office Hadley Centre, UK	$1.9° \times 1.3°$	[37]
IPSL-CM5A-LR	Institute Pierre-Simon Laplace, France	$3.8° \times 1.9°$	[38]

2.3. The Metrocount of Surveying Traffic

The Metrocount tool was established in Australia over 25 years ago aim to deliver the most reliable and sustainable technology for monitoring road traffic, bicycles, and people.

Metrocount traffic data is renowned for its accuracy, flexibility, and variety [39]. This device has been used by over 115 countries across the globe to solve traffic problems and obtain traffic monitoring solutions with a wide range of portable and permanent systems, remote access add-on, and free analysis software. The most popular traffic monitoring system uses two pneumatic tubes, and records every axle to give vehicle volume, speed, and classification data [40]. All Metrocount traffic survey systems are a co-dependent, intelligent combination of robust hardware and world-leading software. MTE™ software plays a crucial role during the initial set-up of the counter classifier, as well as later on, when verifying the system's performance and analyzing the collected data [41]. Figure 3 shows the equipment of Metrocount.

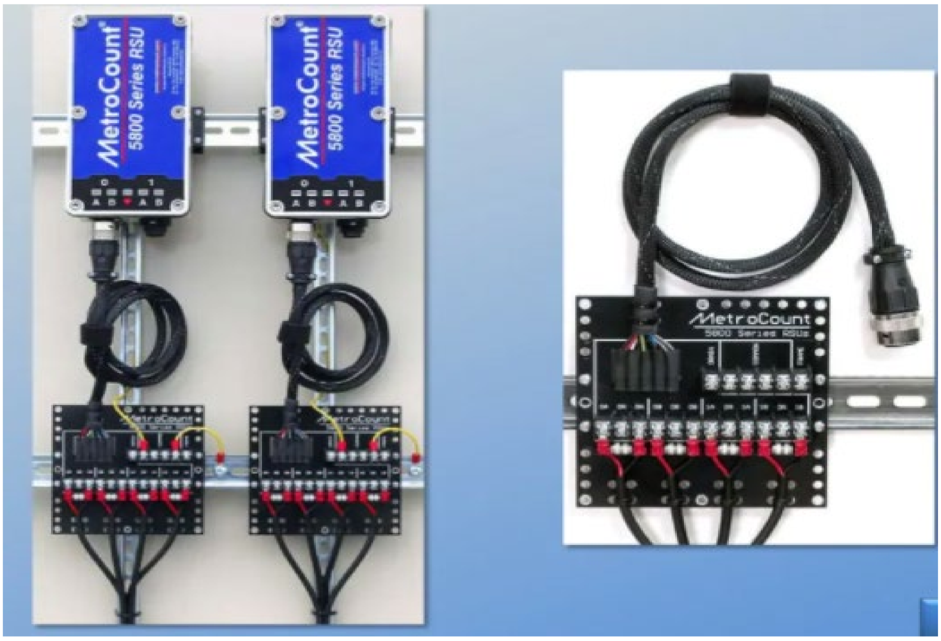

Figure 3. Metrocount equipment.

2.4. Rainfall Harvesting Methods

Instead of letting rainfall flow off, rainwater harvesting involves gathering it and storing it for later use on-site. These retained liquids are used for a variety of tasks, including irrigation and gardening. Broadly, there are two ways of harvesting rainwater: rooftop rainwater harvesting and surface runoff harvesting. Surface runoff harvesting is applied in the urban area, where rainwater flows away as surface runoff. This runoff could be caught and used for recharging aquifers by adopting appropriate methods. On the other hand, rooftop rainwater harvesting is a method of catching rainwater where it falls. In this method, the roof of the house or building serves as the catchment area, and the rainwater is collected from there. It can be either diverted to an artificial recharge system or kept in a tank. If used correctly, this technology, which is less expensive and very successful, contributes to raising the local groundwater level. This technique works best in an urban setting, where rainwater that is collected and stored during rainstorms flows along the ground. To store the surface runoff, the flow of tiny tributaries of rivers or reservoirs is changed. The surface runoff is held in ponds, tanks, and reservoirs designed for this purpose. Effective water conservation techniques are used to store rainwater while lowering evaporation. To maintain clean and healthy water, several steps are taken [42]. In this paper the rational equation for runoff is applied as:

$$Q = 0.0028 \times A \times c \times I \quad (1)$$

where Q = quantity of storm water in m^3/s (0.0028 is the conversion constant to convert FPS units to SI), c = coefficient of runoff (0.35–0.9), according to the type of surface (road pavement) = 0.9, I = intensity of rainfall in mm/h, and A = drainage area in hectares. Time of concentration (T_c) [43] is the amount of time needed for water to flow from the farthest point in the area to the outlet once the soil has become saturated and small depressions have filled, or it is the lag (the amount of time that passes between the start of runoff from a rainfall event over a watershed and when runoff reaches its peak). For design reasons, the duration of a storm at any particular intensity that is expected to occur at any given moment corresponds to the time of concentration. The Kirpich formula [44] is frequently used to compute Tc as a function of slope and slope length:

$$T_c = 0.0195 L^{0.77} S^{-0.385} \tag{2}$$

where S is the watershed gradient (m/m), which is derived as the difference in elevation between source and outflow divided by length, T_c is the time of concentration (min), and L is the maximum length of flow (m). In order to use surface runoff in irrigation or domestic uses, harvesting rainwater by well recharging is applied according to the equation. The design of the recharge well was created based on three key points, i.e., (i) to the well location, (ii) the available space, and (iii) the design discharge (Q), the value of Q was calculated using Equation (1), given that the length of the road is 12 km, and the width is 3.65 m. In this study, for a T_c = 15 min, rainfall intensity of 75 mm/hr, and the total runoff volume collected at the ponding site is 300 m^3 (the pond area is 1200 m^2).

Artificial Aquifer Recharge

Gale [45] goes into great detail explaining a variety of artificial aquifer recharge techniques. In essence, it depends on the technique being used for recharging, as well as the geologic and geographic features of the region. The key restriction, for instance, is the adequacy of the aquifer in terms of permeability, hydraulic conductivity, storage capacity, transmissivity, and water quality for deep infiltration via boreholes and wells that pump water into a deep aquifer. For deep infiltration, physical geography is far less crucial; the same strategy can be applied wherever there is the terrain. In this study, the recharging well flow (Q_W) obtained by a constant head recharge on a bore well is given by:

$$Q_W = 2.75 \times d \times h \times k \tag{3}$$

where k is the coefficient of permeability. In this study, the current k is 45 m/d, but a factor of safety of 120% was considered; therefore, the design k = 36 m/d, h is the depth of the pervious sand layer measured from the ground level (20 m), and d is the recharge well (m) = 0.3 m. Based on Equation (3), Q_W = 25 m^3/hr.

3. Results

3.1. Effect of Climate Changes on Road Traffic

As indicated in Figure 4, which serves as the baseline, a statistical analysis was conducted to determine the average monthly rainfall rates in the research area for the years 2008 to 2020. Figure 5 depicts January rainfall scenarios for RCP 4.5 for the years 2024, 2060, 2080, and 2100 with values of 50, 90, 102, 104, and 110 mm/day, respectively. However, for the RCP 8.5 emission for January, the average daily rainfall is 51, 90, 102.5, 105, and 110 mm for the years 2020, 2040, 2060, 2080, and 2100, respectively.

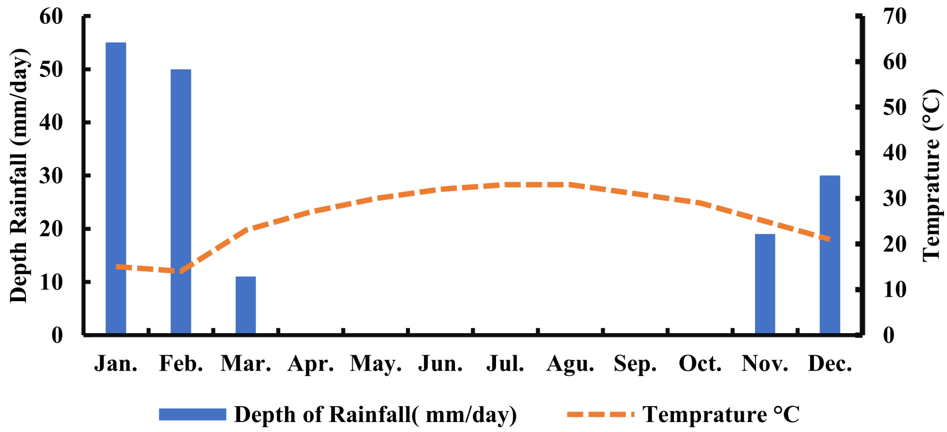

Figure 4. Average data of rainfall depth and temperature in the study area for the period from 2008 to 2020.

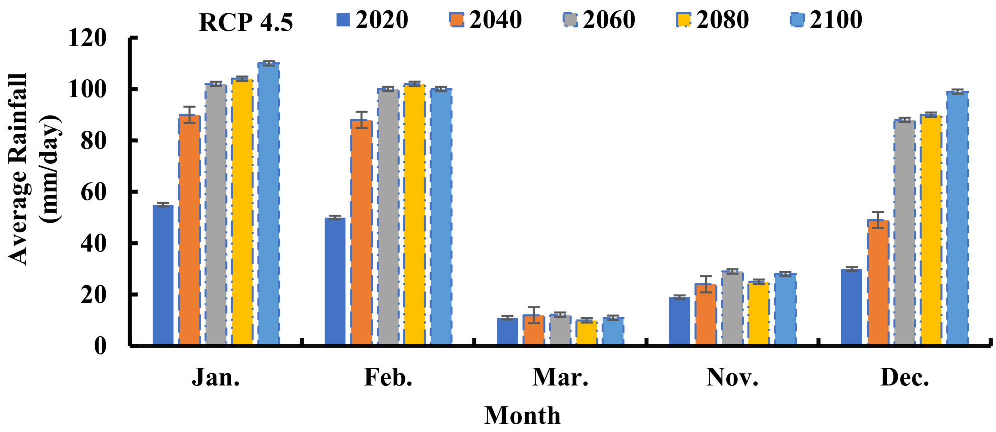

(**A**)

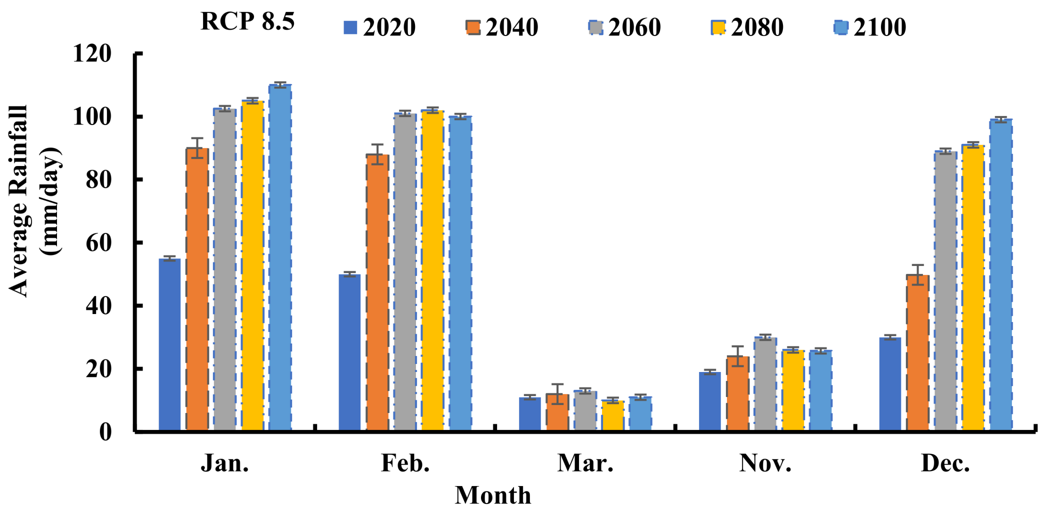

(**B**)

Figure 5. Global average rainfall depth indices over land as simulated at stations in the study area, (**A**) RCP 4.5, and (**B**) RCP 8.5.

3.2. Effect of Rainfall on Traffic Flow

Table 3 shows the average daily (7 a.m. to 5 p.m.) traffic characteristics under the influence of various weather conditions, particularly the effect of rain on the speed of cars and road density, as well as free flow. The data showed that rain lowered the capacity by 2–32%, even if the mean speed decreased. Capacity declines with increases in rainfall intensity. In addition, when the severity of the rain increases, speed diminishes, and the change in speed with respect to dry conditions is 30.8%.

Table 3. Measured Metrocount average daily (7 a.m. to 5 p.m.) traffic characteristics under the influence of various weather conditions.

Condition	Traffic Count (Vehicles)	Average Volume (veh/h)	Capacity (pce)	Mean Speed (km/hr)	Free Flow Speed (km/hr)	Change in Speed (%) with Respect to Dry Condition
Dry condition	7430	630	1375	65	70	-
Wet condition	4670	657	1230	45	55	30.8

Veh, vehicle; pce, passenger car equivalents.

3.3. Speed Analysis

Travel Speed in Rainy Conditions

To assess the travel speed in rainy conditions, in our case study (Cairo Autostorad highway), we compared the average speed in km/hr and associated traffic volume per hour (veh/h) for the normal weather conditions on 28 October 2016 and heavy rain conditions on 20 January 2017. Due to the changing nature of rainfall intensity, the observation period was repeatedly extended. Three time periods were considered: morning peak hours, evening peak hours, and off-peak hours. Table 4 summarizes the features of the traffic flow of the Cairo Autostorad highway under various weather situations. Therefore, the results show that the average speeds are 30, 34, and 50 km/h during the heavy rains in the morning, evening, and off peaks times, respectively. Compared to dry conditions, a decrease of 40, 38, and 28.6% in the average speed is detected for the morning, evening, and off-peak hours, respectively. In addition, the corresponding traffic volumes are 1002, 1350, and 900 veh/h during the heavy rains in the morning, evening, and off-peaks times, respectively, compared to dry conditions, which is a decrease of 70.7, 68, and 59.5% in the average traffic volumes detected for the morning, evening, and off-peak hours, respectively. Figure 6 shows the average depth of rainfall and the speed distribution. in the winter season; the recorded speed distributions are 40, 48, 55, and 60 km/h in January, December, February, and November, respectively. On the other hand, in the dry months of April, May, June, July, August, September, and October, the speed distribution ranges between 65–80 km/h. The relationship between the average speed of the vehicles and the average depth of the rainfall for the Autostorad Cairo Highway in the period from 2008 to 2020 in the winter season is shown in Figure 7. Therefore, the trendline shows an exponential function for rainfall depth and the traffic speed as

$$y = 143.12\, e^{-0.015x} \tag{4}$$

where y is the speed in km/h and x in the rainfall depth in mm, with a determination factor of $R^2 = 0.7076$.

Table 4. Features of traffic flow of the Cairo Autostorad highway under various weather situations.

Time Period	Morning Peak		Evening Peak		Off-Peak	
Weather condition	Heavy rain	Dry condition	Heavy rain	Dry condition	Heavy rain	Dry condition
Average speed (km/h)	30	50	34	55	50	70
Volume per hour (veh/h)	1002	3425	1350	4220	900	2225

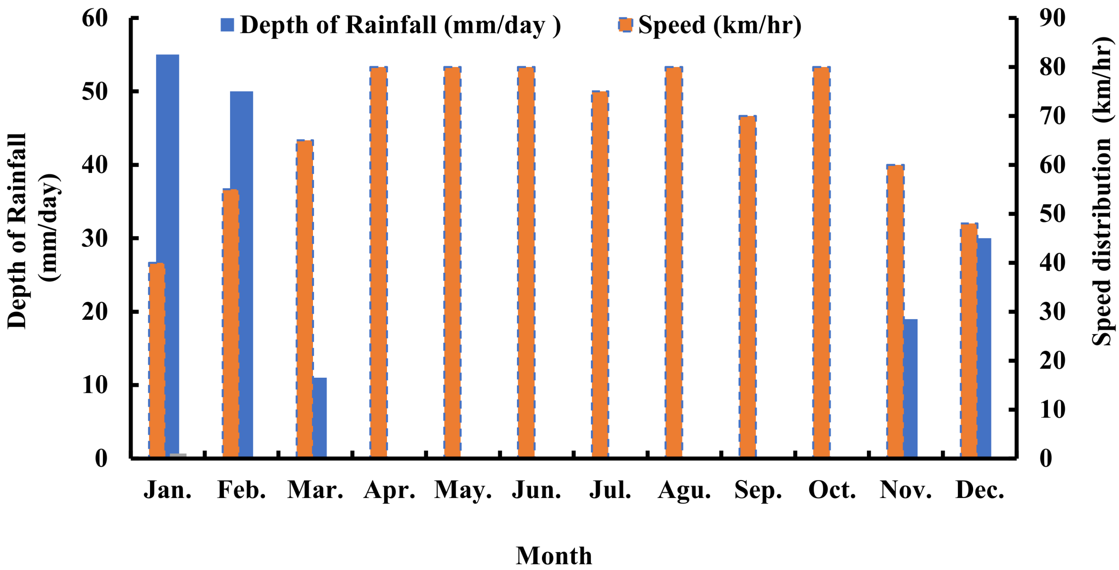

Figure 6. Cairo Autostorad highway average depth of rainfall and speed distribution.

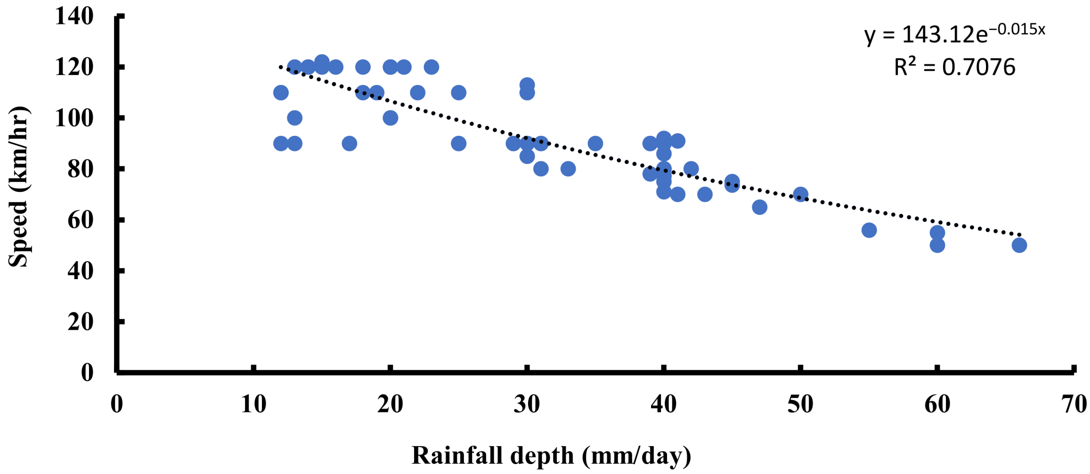

Figure 7. The relationship between the average rainfall depth and the average speed during the period (2008–2020) during the rainy months.

Using Equation (2) and the given depth of rainfall for the years 2040, 2060, 2080, and 2100 for RCP 4.5 and RCP 8.5, the computed speeds are summarized in Table 5. The results show that the speed of the vehicles decreased and the efficiency of the road consequently decreased, compared to the average of the year 2020. The annual loads summarized in this paper were selected from a database of the General Authority for Roads, Bridges, and Land Transport. Figure 8 shows the monthly average daily traffic (MADT) during the period 2008 to 2020; therefore, the monthly average daily traffic (MADT) is recorded in February, January, December, and November at values of 13821, 14123, 14225, and 15,100, respectively. On the other hand, in the dry months (April, May, June, July, August, September, and October) the MADT ranged between 17,260 and 30,325.

Table 5. Rainfall depth and speed for the different scenarios, current 2020, RCP 4.5, and RCP 8.5 for the 2040s, 2060s, 2080s, and 2100s.

Scenario	Year	Rainfall Depth (mm/day)					Speed (km/h)				
		Jan.	Feb.	Mar.	Nov.	Dec.	Jan.	Feb.	Mar.	Nov.	Dec.
Current	2020	50	55	10	19	30	68	63	123	108	91
RCP 4.50	2040	90	88	12	24	49	37	38	120	100	69
	2060	102	100	12.2	29	88	31	32	119	93	38
	2080	104	102	10	25	90	30	31	123	98	37
	2100	110	100	11	28	99	27	32	121	94	32
RCP 8.50	2040	90	88	12	24	49.8	37	38	120	100	68
	2060	103	101	13	30	89	31	31	118	91	38
	2080	105	102	10	26	91	30	31	123	97	37
	2100	110	100	11	26	99	27	32	121	97	32

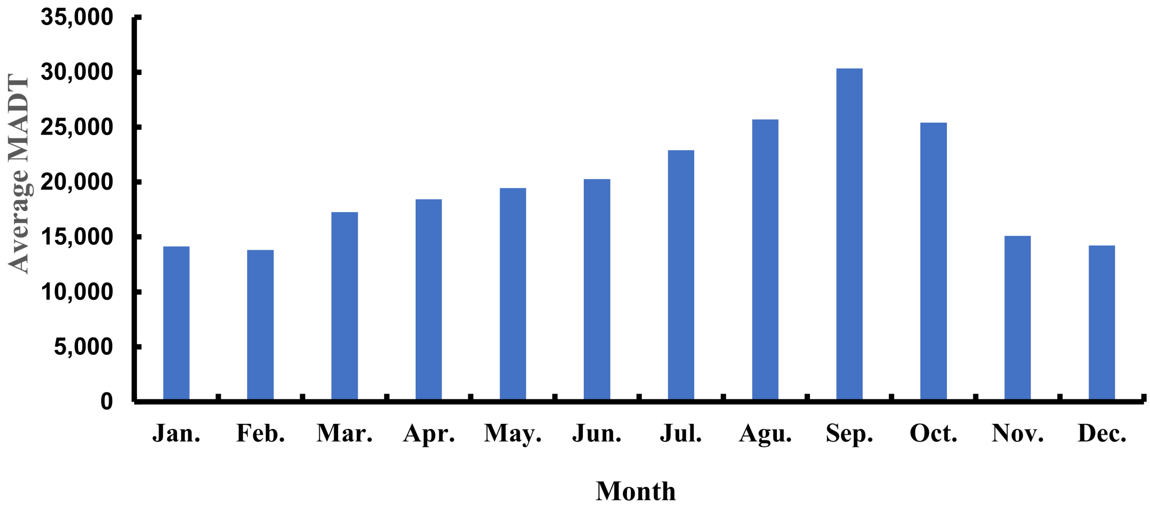

Figure 8. Monthly average daily traffic (MADT) during (2008–2020).

Figure 9 shows the winter season average rainfall depth and highway speed relationship for the current scenario, A: RCP 4.5, and B: RCP 8.5 for the years 2040, 2060, 2080, and 2100. In comparison to the baseline scenario (current), the RCP 4.5 emission scenarios for the years 2040, 2060, 2080, and 2100 predict rainfall depths of 67.8, 126.4, 131.2, and 143.9 mm, with corresponding reductions in highway speed of 23, 34, 35.3, and 36.9%. On the other hand, for the years 2040, 2060, 2080, and 2100, respectively, the RCP 8.5 emission scenarios show a reduction in the highway speed of 23, 34.5, 36.9, and 36.9% due to rain-fall depths of 68.7, 128.4, 143.9, and 143.9 mm, respectively.

3.4. Traffic Flow Reduction at Various Rainfall Densities

According to Figures 6 and 9A,B, rainfall has a significant impact on highway traffic flow characteristics, resulting in varying degrees of speed reductions. Variable rainfall densities, on the other hand, result in varying percentages of reduction. Therefore, we collected data from the same detectors on 28 November 2016, with medium rainfall (roughly 5 mm) and 13 April 2016, with normal weather, as well as on 1 January 2017, with light rainfall (roughly 0.7 mm), and on heavy rainfall day on 27 January 2017. The decrease coefficients of traffic flow characteristics by light, medium, and heavy rainfalls were calculated using detector data collected along the route on many rainy days with varying rainfall densities.

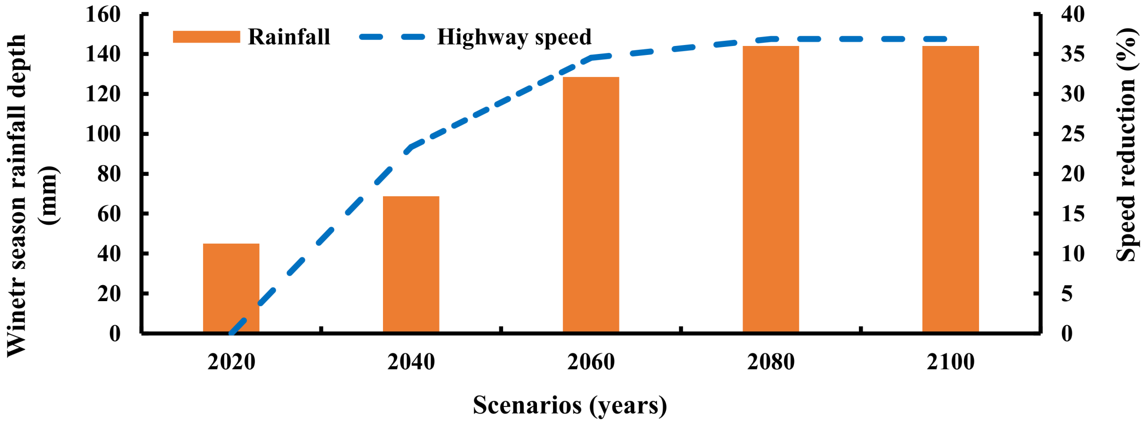

(**A**)

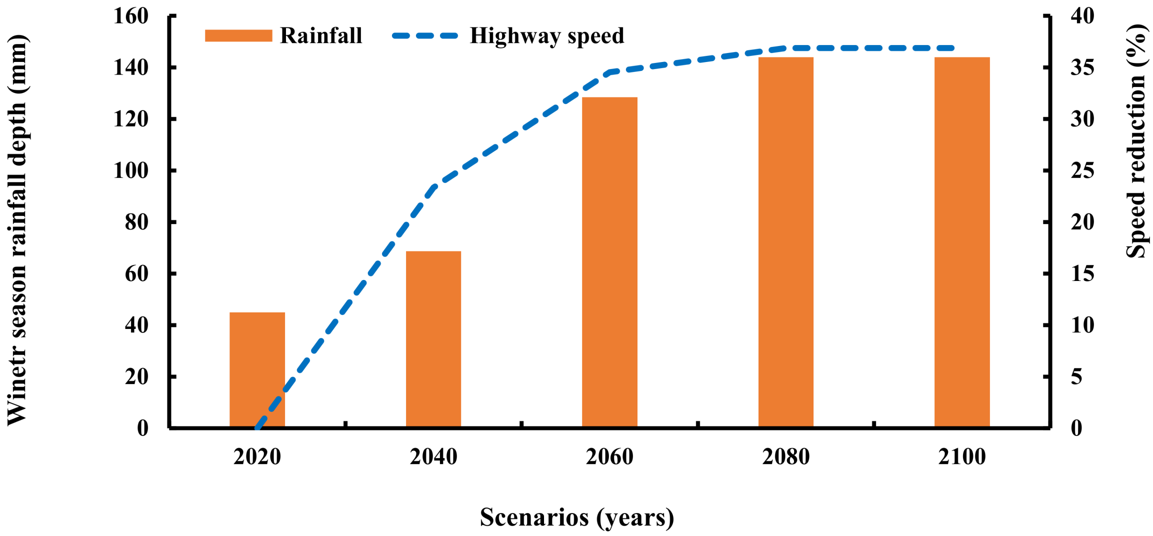

(**B**)

Figure 9. Rainfall depth and highway speed relationship for the current scenario and (**A**): RCP 4.5; (**B**): RCP 8.5 for the years 2040, 2060, 2080, and 2100. (**A**) RCP 4.5 emission scenarios; (**B**) RCP 4.5 emission scenarios.

3.5. Coefficient of Reduction in Heavy Rain

On the day of the rain on 27 January 2017, Cairo was hit by heavy rainfall of more than 18 mm. Comparing the data from the rainy day with the data from the usual day on 28 October 2016, the data from the normal day was used. On both days, the spot speed reductions were investigated using the same volume level data. Because the rainy day occurred on a weekend, the entire day's travel demand was significantly reduced, as a result of the heavy rain, with varying degrees of reduction in different places, due to the low travel demand. In the incomplete dataset, flow rates decreased by 40–60%, demonstrating that users of these highway road portions were highly sensitive to weather conditions, and that the travel demand on these road sections was highly elastic. On the other hand, the volume loss in the other half of the observed routes in the cities was roughly 15% to 25%, indicating a large demand for travel on these route segments. The average reduction in traffic volume was about 40%, which was slightly lower than that of the previous road segments. In addition, using various sets of data with comparable traffic flow levels, the researcher performed a contrast analysis to analyze speed reductions under heavy rain conditions on both days. The data analysis produced the following conclusions: (1) speed reductions vary based on traffic flow levels; (2) the lower the traffic volume, the greater the speed reduction; (3) speeds fell from 15 to 40%, with an average speed loss of about 28% under heavy rain.

3.6. The Subsequent Day after Rain

The traffic performance was calculated using data collected on the next day, following a heavy downpour on numerous roads; there was rain, and the situation had become worse that day because it was a work day, and most passengers had pressing needs to travel for work; therefore, the traffic volume decrease was somewhat smaller than that on the weekend, at 20–50%. Between the peak and off-peak hours, there was little, if any, difference in volume, with both experiencing a 40% decrease. At the same time, the congestion on the highway was reduced. Based on previous data analysis, we may expect the traffic flow characteristics on a heavy rainfall day to have a major impact; however, the highway's traffic conditions do not appear to be substantially worse the next day. Compared to a typical workday, driving speed did not appear to be affected. Based on previous data analysis, we may expect the traffic flow characteristics on a wet day to have a big impact, yet the expressway's traffic conditions do not appear to be substantially worse the next day. The average speed fell by about 28% on a wet day, but only by about 5% the next day.

3.7. Coefficient of Reduction in Lighter Rain

Between November 2016 and January 2017, data was gathered on days with varied rain concentrations to show the diverse impacts on highway traffic flow. The following are the results of the data analysis: (i) drivers will lower their travel demand in the case of bad weather (rainfall greater than 60 mm); (ii) the impact of rain on highway traffic flow is minor with moderate rainfall (precipitation greater than 2.5 mm but less than 10 mm) and light rain (precipitation less than 2.5 mm); (iii) with heavy rainfall (precipitation greater than 60 mm), the impact of rain on highway traffic flow is significant, and the volume and speed of traffic are frequently reduced (see Table 5). Therefore, decreased coefficients of traffic flow characteristics in Egypt may be proposed under various rain densities. Under severe rain, moderate rain, and light rain, the volume reductions on the highways are 40%, 15%, and 5%, respectively, while the average speed reductions are 25, 8, and 0%, respectively.

3.8. Identification of Ponding Sites

To solve the problem of collecting rainwater on the road, which causes disruption to traffic, a survey of the road site was carried out and the places where the water collects were determined, as shown in Figure 10. Figure 11 shows the solutions to this problem, as the water was collected at the lowest level on the road. It was proposed to make a well at these sites to collect rainwater. According to the survey, there are 40 depressed locations that create ponding areas when it rains. However, it is clear from the survey done during the rainy season that there are many important ponding locations in Cairo's commercial and densely populated areas that need to be harvested when it rains. At total of 40 ponds were identified during a survey (Figure 10). This method revealed the longitudinal elevation profile (Figure 11) showing the differences in elevation of the depressed regions. As seen in Figure 10, these low-lying regions flood during periods of severe precipitation. The longitudinal elevation profile analysis became helpful for the verification of ponding depth at identified ponding locations.

3.9. Recommended Recharging Wells

Based on Equation (3) and values of the parameters, the recharging capacity of the well was estimated as 25 m^3/h. At the 40 pond locations, a 30 cm recharging well is recommended to be constructed for rainwater harvesting. The recharging wells will clear the ponding volumes within 2.5 to 3.5 h after the rainfall stops. The layout view of recharge wells is shown in Figure 12. Moreover, the installation of a filter in the well to infiltrate the harvested rainwater to improve its quality is an important issue; the recommended filter thickness is 45 cm, comprised of 30 cm of gravel (size range: 15–25 mm), and 20 cm of fine gravel of (size range: 6–12 mm). The filter should be tested in the field to check its efficiency.

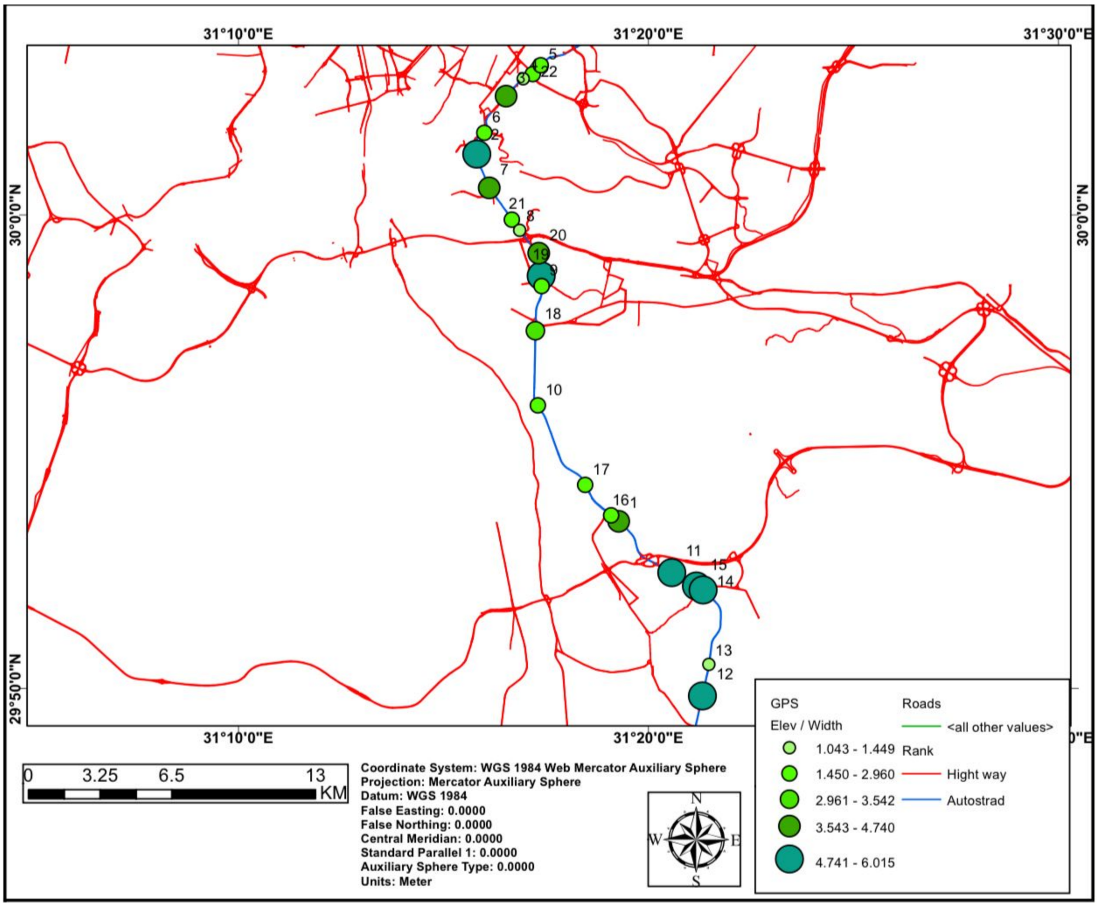

Figure 10. Location of ponding sites and ponding depth.

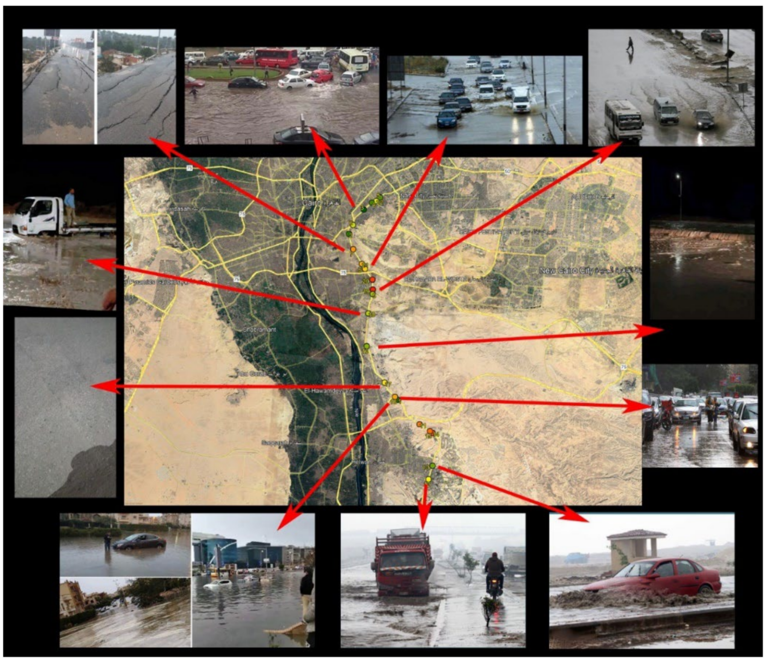

Figure 11. Longitudinal profiles of roads collecting rainwater in Egypt.

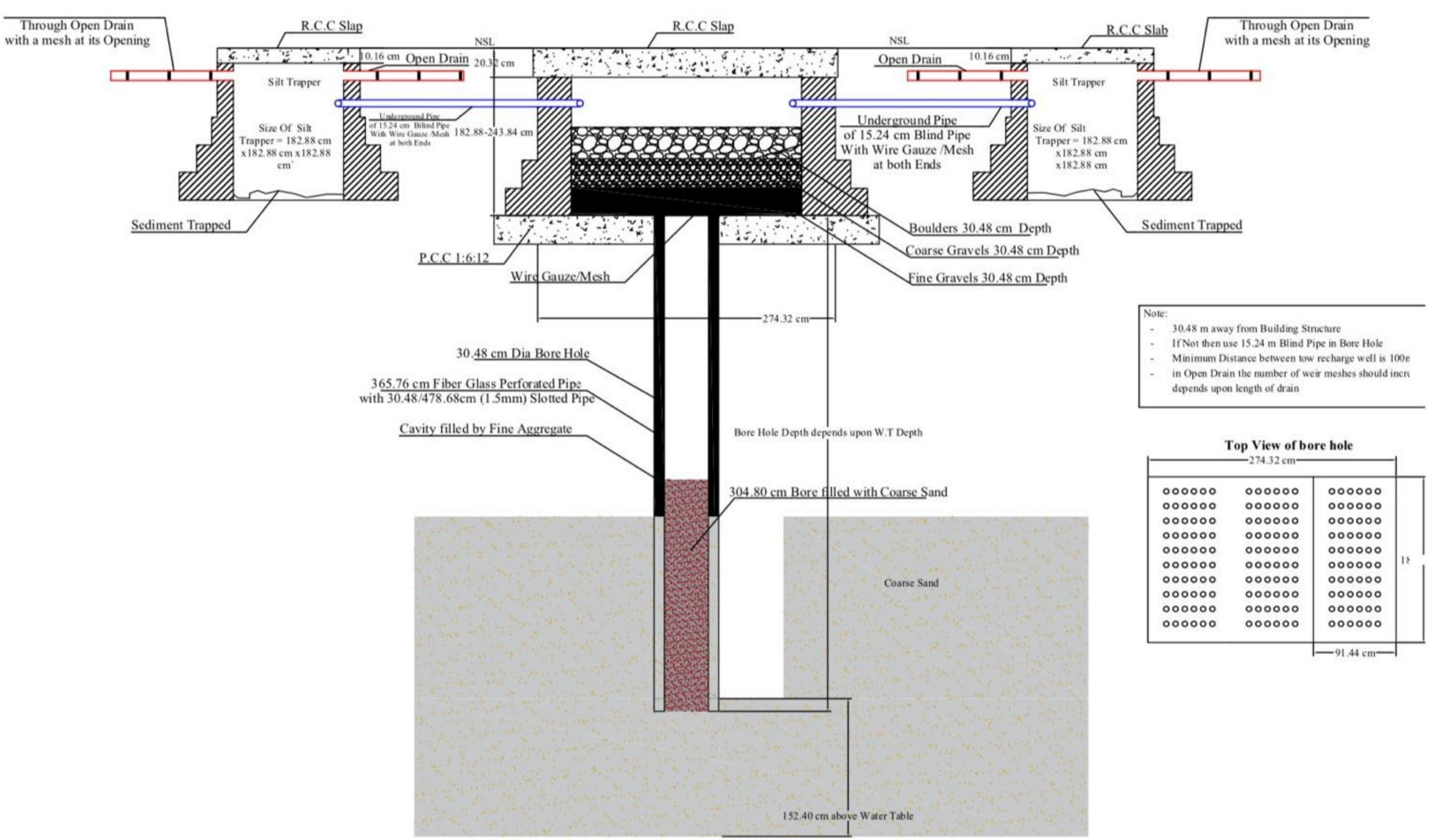

Figure 12. Typical design of a recharge well used for rainwater harvesting.

4. Discussion

4.1. Rainfall–Depth–Vehicle Speed Relationship Compared with Literature

Equation (2) computes the rainfall and vehicle travel speed distribution; the average speeds of 30, 34, and 50 km/h during the heavy rains in the morning, evening, and off-peak times indicate a decrease in the vehicle travel speed by 40, 38, and 28.6%, respectively. In addition, the corresponding traffic volumes decreased by 70.7, 68, and 59.5%, respectively. These results are compatible with the previous literature by [46–48]. According to Luo and Wang [46], the results of the effects of rainfall on the characteristics of freeway traffic flow show that, as the intensity of the rain grows, it has a higher impact on the maximum highway volume and free flow speed. In addition, for light, moderate, and heavy rainfall weather conditions, the maximum traffic flow rate reduces by 15.7%, 19.1%, and 32.5%, respectively, and the free flow speed decreases by 4.4%, 7.3%, and 10.6%, respectively compared to normal weather. When Aksoy and Öğüt [47] looked into how the discharge flow rate changed when it rained on Istanbul's urban motorways, they discovered that there was a difference between sunny and rainy conditions of up to 37% in discharge flow. Rain was shown to have a greater impact on motorway sections with higher free flow speeds (FFS), and the discharge flow reduction was greater in the higher FFS sections than it was for areas with the lowest FFS. For 1 mm/m^2/h of precipitation, when FFS is 84 km/h, the discharge flow is predicted to be 1719 pcu/h/lane, and if FFS is 104 km/h, it is expected to be 1560 pcu/h/lane. In addition, the impact of rainfall intensity on the heteroscedastic traffic speed dispersion on urban highways in Hong Kong was modelled by Jian et al. [48]. They concluded that the speed dispersion of vehicular traffic was measured using the coefficient of variation of speed (cVS), and the investigation demonstrates that, at various traffic densities and rainfall intensities, the empirical values of cVS typically vary from 0.05 to 0.2, and that the exponential function offers a good match to the traffic speed data in both dry and wet situations. In addition, according to [49–51], the reduction in speed caused by rainfall is 77, 40, and 37 km/hr for rainfall depths of 78, 116, and 125 mm, respectively.

4.2. Rainwater Harvesting by Recharging Wells

The proposed harvesting rainwater system using a researching well is a new technology, and careful consideration should be taken in order to create a successful system, as reported by Salameh et al. [52]. In Jordan's managed aquifer recharge (MAR) design and implementation: (1) The purpose of the managed aquifer recharge includes (i) the seasonal or long-term storage of water, (ii) the building or augmenting of reserves, (iii) recharge as a means of additional water quality treatment, (iv) the prevention of aquifer subsidence, (v) the improvement of water quality by dilution, (vi) the prevention of saltwater intrusion and groundwater salinization; (2) The availability of suitable water for recharge includes: (i) The timing and reliability of supply quantity, (ii) the distance and elevation change from areas of water use, and (iii) the water quality of the supply; (3) The conditions in the receiving aquifer includes: (i) available land in locations with suitable physical conditions, (ii) the quality of recharge water after pretreatment, (iii) the potential geohydro-chemical interactions, and (iv) the rechargeability and withdrawal of well yields; (4) The facility conditions involves: (i) access to roads, energy, and communications, and (ii) the institutional capacity to control the site; (5) MAR infrastructure required as part of the pre-recharge process includes: (i) filtration, (ii) sediment removal, and (iii) chemical conditioning, (iv) other recharge methods, such as wells, surface spreading, recharge pools, or channels, and (v) extractions methods, such as wells, galleries, flow to a stream or spring, and post-extraction treatment needs; (6) socioeconomic conditions, including: (i) end-user acceptance of water, (ii) economic conditions, (iii) institutional capacity to design, construct, operate, and maintain the MAR project, and (iv) the availability of alternative supplies or storage and treatment options. A significant problem with mapping MAR is combining various datasets with geographic information systems (GIS). A multi-criteria decision analysis (McDA) is frequently employed for difficult judgments, including various aspects identified by Malczewski and Rinner [53]. The methods remain highly arbitrary and depend on expert judgement, but the scoring and weighting of various factors are formalized so that they can be easily expanded and updated as new information becomes available, factors are added, or circumstances change to the point where scores and weights need to be replaced. In order to choose locations for rainwater collection, Ibrahim et al. [42] identified potential locations for rainwater conservation and the construction of nine dams in appropriate places; potential sites for rainwater conservation in the Dohuk governorate were identified using remote sensing data and the generated GIS-based suitability model.

5. Conclusions and Recommendations

The expected climate change will have a detrimental effect on the economy, increase the frequency of flooding, and endanger public safety. Traditional road assessment techniques were deemed ineffective due to complete flooding; hence no adequate investigation was carried out. This study assessed the reduction in traffic flow characteristics on the highway due to rainfall depth in the winter season, and proposed a design approach for rainwater harvesting by researching wells to solve the traffic problems and convert the runoff to a groundwater resource that can be utilized in irrigation and domestic uses. The Cairo Autostorad highway in Egypt was taken as a case study. The studied road is about 12 km long, and about 40 water ponds exist on the road; for each pond, a 30 cm recharging well, with a maximum recharging capacity of 25 m^3/h with satisfactory performance, is recommended to be constructed for rainwater harvesting. The recharging wells will clear the volume of the ponds within 2.5 to 3.5 h after the rainfall stops. The design incorporates a 1.2 safety factor against the recharging well blockage. In order to restore the recharge rate before the winter season, the well must also be developed by surging or jetting. Additionally, for optimum infiltration of rainwater, recharge chambers must be regularly operated and maintained. Moreover, the findings indicated that the relationship between the average rainfall depth and the average speed measured by the Metrocount tool during the period 2008–2020 during rainy months is modeled by an exponential function of a determining factor of $R^2 = 0.7076$. For the current scenario (2020), the average depth of the winter rainfall was 45 mm, and the average highway speed was 78 km/h. In the future, compared to the baseline scenario (current), the RCP 4.5 emission scenarios for the years 2040, 2060, 2080, and 2100 predict rainfall depths of 67.8, 126.4, 131.2, and 143.9 mm, respectively, with corresponding reductions in highway speeds of 23, 34, 35.3, and 36.9%, respectively. On the other hand, for the years 2040, 2060, 2080, and 2100, respectively, the RCP 8.5 emission scenarios show a reduction in the highway speed of 23, 34.5, 36.9, and 36.9%, respectively, due to rainfall depths of 68.7, 128.4, 143.9, and 143.9 mm, respectively. The results of the study's comparison of rainfall depth and corresponding reductions in traffic speed to the results in the literature show a good level of agreement. This study identified that rainwater harvesting using recharging wells is an alternative freshwater source for sustainable water resource management, as well as a method for solving the traffic problems in urban areas.

Author Contributions: Conceptualization, M.E.G. and A.M.E.S.; methodology, A.M.E.S. and M.E.G.; software, M.E.G. and H.B.F.; formal analysis, A.M.E.S. and H.B.F.; investigation, H.B.F.; data curation, A.M.E.S. and H.B.F.; writing—original draft preparation, M.E.G.; writing—review and editing, A.M.E.S.; supervision M.E.G. All authors have read and agreed to the published version of the manuscript.

Funding: This research received no external funding.

Institutional Review Board Statement: Not applicable.

Informed consent Statement: Not applicable.

Data Availability Statement: Not applicable.

Acknowledgments: We thank the engineering staff of the Civil Aviation Authority and Meteorological Authority in Egypt for providing our climate data. In addition, we thank the anonymous reviewers and the editors for their very supportive comments.

Conflicts of Interest: The authors declare no conflict of interest.

References

1. Singh, C.; Madhavan, M.; Arvind, J.; Bazaz, A. Climate change adaptation in Indian cities: A review of existing actions and spaces for triple wins. *Urban Clim.* **2021**, *36*, 100783. [CrossRef]
2. Walter, L.F.; Abdul-Lateef, B.; Olawale, E.O.; Ulisses, M.A.; Desalegn, Y.A.; Pastor, D.C.M.; Gustavo, J.N.; Paulette, B.; Otienoh, O.; Yannick Toamukum, N.; et al. Assessing the impacts of climate change in cities and their adaptive capacity: Towards transformative approaches to climate change adaptation and poverty reduction in urban areas in a set of developing countries. *Sci. Total Environ.* **2019**, *692*, 1175–1190.
3. Liu, Y.; Zou, Y.; Wang, Y.; Wu, B. Impact of fog conditions on lane-level speeds on freeways. *J. Transp. Eng. Part A Syst.* **2020**, *146*, 04020095. [CrossRef]
4. Han, G.; Pepin, P. Introduction to the Special Section on the aquatic climate change adaptation services program. *Atmos. Ocean.* **2019**, *57*, 1–2. [CrossRef]
5. Aalbers, C.B.E.M.; Coninx, I.; Swart, R.J. Identification of Relevant International Networks, Programmers and Institutions for JPI Climate Research. 2018 Work Package 3-Deliverable 3.1. SINcERE. Available online: www.jpi-climate.eu (accessed on 10 June 2022).
6. Wilson, C.; Guivarch, C.; Kriegler, E.; Van Ruijven, B.; Van Vuuren, D.P.; Krey, V.; Thompson, E.L. Evaluating process-based integrated assessment models of climate change mitigation. *Clim. Change* **2021**, *166*, 1–22. [CrossRef]
7. Gidden, M.J.; Riahi, K.; Smith, S.J.; Fujimori, S.; Luderer, G.; Kriegler, E.; Takahashi, K. Global emissions pathways under different socioeconomic scenarios for use in CMIP6: A dataset of harmonized emissions trajectories through the end of the century. *Geosci. Model Dev.* **2019**, *12*, 1443–1475. [CrossRef]
8. Stouffer, R.J.; Eyring, V.; Meehl, G.A.; Bony, S.; Senior, c.; Stevens, B.; Taylor, K.E. CMIP5 scientific gaps and recommendations for CMIP6. *Bull. Am. Meteorol. Soc.* **2017**, *98*, 95–105. [CrossRef]
9. Yang, X.; Yu, X.; Wang, Y.; He, X.; Pan, M.; Zhang, M.; Sheffield, J. The optimal multi-model ensemble of bias-corrected CMIP5 climate models over China. *J. Hydrometeorol.* **2020**, *21*, 845–863. [CrossRef]
10. Gabr, M.E. Management of irrigation requirements using FAO-CROPWAT 8.0 model: A case study of Egypt. *Modeling Earth Syst. Environ.* **2021**, 1–16. [CrossRef]
11. Ministry of Water Resources and Irrigation (MWRI). *Egypt's Water Resources Plan for 2017–2037*; Planning Sector, Ministry of Water Resources and Irrigation (MWRI): Giza, Egypt, 2017. Available online: https://www.mwri.gov.eg (accessed on 10 January 2022). (In Arabic)
12. Mostafa, S.M.; Wahed, O.; El-Nashar, W.Y.; El-Marsafawy, S.M.; Abd-Elhamid, H.F. Impact of climate change on water resources and crop yield in the Middle Egypt region. *AQUA Water Infrastruct. Ecosyst. Soc.* **2021**, *70*, 1066–1084. [CrossRef]
13. Gabr, M.E. Modelling net irrigation water requirements using FAO-CROPWAT 8.0 and CLIMWAT 2.0: A case study of Tina Plain and East South ElKantara regions, North Sinai, Egypt. *Arch. Agron. Soil Sci.* **2021**, *68*, 1322–1337. [CrossRef]
14. Hafizi Md Lani, N.; Yusop, Z.; Syafiuddin, A. A review of rainwater harvesting in Malaysia: Prospects and challenges. *Water* **2018**, *10*, 506. [CrossRef]
15. Ruso, M.; Akıntuğ, B.; Kentel, E. Optimum tank size for a rainwater harvesting system: Case study for Northern cyprus. *Earth Environ. Sci.* **2019**, *297*, 012026. [CrossRef]
16. Gabr, M.; El-Ghandour, H.; Elabd, S. Rainwater Harvesting from Urban coastal cities Using Recharging Wells: A case Study of Egypt. *Port-Said Eng. Res. J.* **2022**, *in press*. [CrossRef]
17. Zabidi, H.A.; Goh, H.W.; Chang, C.K.; Chan, N.W.; Zakaria, N.A. A review of roof and pond rainwater harvesting systems for water security: The design, performance and way forward. *Water* **2020**, *12*, 3163. [CrossRef]
18. Gado, T.A.; El-Agha, D.E. Feasibility of rainwater harvesting for sustainable water management in urban areas of Egypt. *Environ. Sci. Pollut. Res.* **2020**, *27*, 32304–32317. [CrossRef]
19. Tolossa, T.T.; Abebe, F.B.; Girma, A.A. Review: Rainwater harvesting technology practices and implication of climate change characteristics in Eastern Ethiopia. *Cogent Food Agric.* **2020**, *6*, 1724354. [CrossRef]
20. Min, Z.; Yufu, L.; Wenqi, S.; Yixiong, X.; Chang, J.; Yong, W.; Yuqi, B. Impact of rainfall on traffic speed in major cities of China. *Sustainability* **2021**, *13*, 9074. [CrossRef]
21. Gabr, M.E. Design methodology for sewage water treatment system comprised of Imhoff's tank and a subsurface horizontal flow constructed wetland: A case study Dakhla Oasis, Egypt. *J. Environ. Sci. Health Part A* **2022**, *57*, 52–64. [CrossRef]
22. Madleen, S.; Gabr, M.E.; Mohamed, M.; Hani, M. Random Forest modelling and evaluation of the performance of a full-scale subsurface constructed wetland plant in Egypt. *Ain Shams Eng. J.* **2022**, *13*, 101778.
23. Hofman-Caris, R.; Bertelkamp, C.; de Waal, L.; van den Brand, T.; Hofman, J.; van der Aa, R.; van der Hoek, J.P. Rainwater harvesting for drinking water production: A sustainable and cost-effective solution in the Netherlands. *Water* **2019**, *11*, 511. [CrossRef]
24. El Afandi, G.; Morsy, M. Developing an early warning system for flash flood in Egypt: Case study Sinai Peninsula. In *Flash Floods in Egypt*; Springer: Cham, Switzerland, 2020; pp. 45–60.
25. Vidas, M.; Tubić, V.; Ivanović, I.; Subotić, M. One Approach to Quantifying Rainfall Impact on the Traffic Flow of a Specific Freeway Segment. *Sustainability* **2022**, *14*, 4985. [CrossRef]

26. Yang, Y.; Ng, S.T.; Dao, J.; Zhou, S.; Xu, F.J.; Xu, X.; Zhou, Z. BIM-GIS-DcEs enabled vulnerability assessment of interdependent infrastructures—A case of stormwater drainage-building-road transport Nexus in urban flooding. *Autom. Constr.* **2021**, *125*, 103626. [CrossRef]
27. Shahdani, F.J.; Ariza, M.P.S.; Coelho, M.R.F.; Sousa, H.S.; Matos, J.C. The indirect impact of flooding on the road transport network, a case study of Santarém region in Portugal. In Proceedings of the 30th European Safety and Reliability Conference and the 15th Probabilistic Safety Assessment and Management Conference, Angers, France, 19–23 September 2021.
28. Yoo, B.H.; Kim, J.; Lee, B.W.; Hoogenboom, G.; Kim, K.S. A surrogate weighted mean ensemble method to reduce the uncertainty at a regional scale for the calculation of potential evapotranspiration. *Sci. Rep.* **2020**, *10*, 1–11. [CrossRef]
29. Broggio, M.F.; Garcia, C.A.E.; Silva, R.R.D. Evaluation of South Atlantic Thermohaline Properties from BESM-OA2. 5 and Three Additional Global Climate Models. *Ocean Coast. Res.* **2021**, *69*. [CrossRef]
30. Rehman, N.; Adnan, M.; Ali, S. Assessment of CMIP5 climate models over South Asia and climate change projections over Pakistan under representative concentration pathways. *Int. J. Glob. Warm.* **2018**, *16*, 381–415. [CrossRef]
31. Shen, C.; Duan, Q.; Miao, C.; Xing, C.; Fan, X.; Wu, Y.; Han, J. Bias. Correction and ensemble projections of temperature changes over ten subregions in CORDEX East Asia. *Adv. Atmos. Sci.* **2020**, *37*, 1191–1210. [CrossRef]
32. Xu, Y.; Gao, X.; Giorgi, F.; Zhou, B.; Shi, Y.; Wu, J.; Zhang, Y. Projected changes in temperature and precipitation extremes over China as measured by 50-yr return values and periods based on a CMIP5 ensemble. *Adv. Atmos. Sci.* **2018**, *35*, 376–388. [CrossRef]
33. Dix, M.; Vohralik, P.; Bi, D.; Rashid, H.; Marsland, S.; O'Farrell, S.; Puri, K. The ACCESS coupled model: Documentation of core CMIP5 simulations and initial results. *Aust. Meteorol. Oceanogr. J.* **2013**, *63*, 83–99. [CrossRef]
34. Mabhaudhi, T.; Chibarabada, T.P.; Chimonyo, V.G.P.; Modi, A.T. Modelling climate change impact: A case of bambara groundnut (*Vigna subterranea*). *Phys. Chem. Earth Parts A/B/C* **2018**, *105*, 25–31. [CrossRef]
35. Fumière, Q.; Déqué, M.; Nuissier, O.; Somot, S.; Alias, A.; Caillaud, C.; Seity, Y. Extreme rainfall in Mediterranean France during the fall: Added value of the CNRM-AROME Convection-Permitting Regional Climate Model. *Clim. Dyn.* **2020**, *55*, 77–91. [CrossRef]
36. Creese, A.; Washington, R. A process-based assessment of CMIP5 rainfall in the Congo Basin: The September–November rainy season. *J. Clim.* **2018**, *31*, 7417–7439. [CrossRef]
37. Dong, Y.; Armour, K.C.; Proistosescu, C.; Andrews, T.; Battisti, D.S.; Forster, P.M.; Shiogama, H. Biased estimates of equilibrium climate sensitivity and transient climate response derived from historical CMIP6 simulations. *Geophys. Res. Lett.* **2021**, *48*, e2021GL095778. [CrossRef]
38. Sepulchre, P.; Caubel, A.; Ladant, J.B.; Bopp, L.; Boucher, O.; Braconnot, P.; Brockmann, P.; Cozic, A.; Donnadieu, Y.; Dufresne, J.L.; et al. IPSL-cM5A2-an Earth system model designed for multi-millennial climate simulations. *Geosci. Model Dev.* **2020**, *13*, 3011–3053. [CrossRef]
39. Goyal, T. Traffic Data Analysis Using Automatic Traffic Counter-Cum-Classifier. *Indian J. Sci. Technol.* **2016**, *9*, 1–4. [CrossRef]
40. Puan, O.C.; Nor, N.S.M.; Mashros, N.; Hainin, M.R. Applicability of an automatic pneumatic–tube–based traffic counting device for collecting data under mixed traffic. *Earth Environ. Sci.* **2019**, *365*, 012032. [CrossRef]
41. José Manuel, V.; Paola carolina, B. *Chapter Two—Sustainability Assessment of Transport Policies, Plans and Projects*; Mouter, N., Ed.; Advances in Transport Policy and Planning; Academic Press: cambridge, MA, USA, 2021; Volume 7, pp. 9–50.
42. Ibrahim, G.R.F.; Rasul, A.; Ali Hamid, A.; Ali, Z.F.; Dewana, A.A. Suitable site selection for rainwater harvesting and storage case study using Dohuk Governorate. *Water* **2019**, *11*, 864. [CrossRef]
43. John, P.; Bahram, G.; Ramesh, R. Reference time of concentration estimation for ungauged catchments. *Earth Sci. Res.* **2018**, *7*, 58–73.
44. Kirpich, Z.P. Time of concentration of small agricultural watersheds. *J. Civ. Eng.* **1940**, *10*, 362.
45. Gale, I. Strategies for Managed Aquifer Recharge (MAR) in Semi-arid Areas. 2005. UNESCO, IHP/2005/GW/MAR 30p. Available online: https://unesdoc.unesco.org/ark:/48223/pf0000143819 (accessed on 15 June 2022).
46. Wang, Y.; Luo, J. Study of Rainfall Impacts on Freeway Traffic Flow characteristics. World conference on Transport Research—WCTR 2016 Shanghai. *Transp. Res. Procedia* **2017**, *25*, 1533–1543.
47. Aksoy, G.; Öğüt, K.S. Discharge flow rate change under rainy conditions on Urban Motorways. *Promet—Traffic Transp.* **2018**, *30*, 733–744. [CrossRef]
48. Jian, L.; William, H.K.L.; AScE, M.; Xingang, L. Modeling the effects of rainfall intensity on the heteroscedastic traffic speed dispersion on urban Roads. *J. Transp. Eng.* **2016**, *142*, 05016002. [CrossRef]
49. Ong, G.P.; Fwa, T.F. Hydroplaning risk management for grooved pavements. In Proceedings of the 7th International Conference on Managing Pavement Assets, calgary, AB, canada, 23–28 June 2008.
50. Galatioto, F.; Glenis, V.; Roberts, R.; Kilsby, C. Exploring and modelling the impacts of rainfall and flooding on transport network. The case study of Newcastle upon Tyne. In Proceedings of the 2nd International Conference on Urban Sustainability and Resilience (USAR 2014), London, UK, 5–7 September 2014.
51. YouTube. Video: UK Flood Observation, Perth. 2012. Available online: https://www.youtube.com/watch?v=tcqEARMI-_k (accessed on 22 June 2022).

52. Salameh, E.; Abdallat, G.; Van der Valk, M. Planning considerations of managed aquifer recharge (MAR) projects in Jordan. *Water* **2019**, *11*, 182. [CrossRef]
53. Malczewski, J.; Rinner, C. *Multicriteria Decision Analysis in Geographic Information Science*; Springer: Berlin, Germany, 2018; 331p. [CrossRef]